

Reorientation in Antiferromagnetic Multilayers: Spin-Flop Transition and Surface Effects

U.K. Rößler^{(a)*} and A.N. Bogdanov^{(a,b)†}

(a) *Leibniz-Institut für Festkörper- und Werkstoffforschung Dresden
Postfach 270116, D-01171 Dresden, Germany and*

*(b) Donetsk Institute for Physics and Technology
83114 Donetsk, Ukraine*

(Dated: February 2, 2008)

Nanoscale superlattices with uniaxial ferromagnetic layers antiferromagnetically coupled through non-magnetic spacers are recently used as components of magnetoresistive and recording devices. In the last years intensive experimental investigations of these artificial antiferromagnets have revealed a large variety of surface induced reorientational effects and other remarkable phenomena unknown in other magnetic materials. In this paper we review and generalize theoretical results, which enable a consistent description of the complex magnetization processes in antiferromagnetic multilayers, and we explain the responsible physical mechanism. The general structure of phase diagrams for magnetic states in these systems is discussed. In particular, our results resolve the long standing problem of a “surface spin-flop” in antiferromagnetic layers. This explains the different appearance of field-driven reorientation transitions in systems like Fe/Cr (001) and (211) superlattices, and in [CoPt]/Ru multilayers with strong perpendicular anisotropy.

PACS numbers: 75.70.-i, 75.50.Ee, 75.10.-b 75.30.Kz

1. Introduction.

Since the discovery of antiferromagnetic interlayer exchange [1], a large variety of magnetic nanostructures consisting of stacks of ferromagnetic layers with antiferromagnetic coupling via spacers has been synthesized. For recent investigations on such superlattices, see [2, 3, 4, 5, 6] and references in [7, 8]. These *synthetic antiferromagnets* are of great interest in modern nanomagnetism, in particular due to their application in spin electronics [9] and high-density recording technologies [10].

In view of their magnetic states and field-induced reorientation transitions, these antiferromagnetically coupled superlattices can be separated into two groups: (1) Systems with magnetization in the film plane and low (higher-order) anisotropies only, e.g., multilayers grown on (001) faces of cubic substrates [3] with a four-fold anisotropy owing to the magneto-crystalline anisotropies of the materials (for further references and a survey of their magnetic properties, see [8]). In these high symmetry systems, magnetic states are mainly determined under competing influence of bilinear and biquadratic exchange interactions and the intrinsic magnetic anisotropy. For this type of multilayers with a fully compensated antiferromagnetic collinear ground state, the magnetization processes generally have a simple character, in particular in the low anisotropy limit no reorientation transition occurs with fields in direction of easy axes [8]. (2) The other group of the synthetic antiferromagnets own an often sizeable *uniaxial* anisotropy. This group includes superlattices with intrinsic or *induced* in-plane uniaxial anisotropy, e.g. multilayers on (110) and (211) faces of cubic substrates [2, 4], or nanostructures with perpendicular anisotropy [5]. Here, an interplay between the uniaxial anisotropy and the confining geometry of the multilayers determines their magnetic properties and gives rise to effects such as *surface spin-flops* [2, 4], field induced cascades of magnetization jumps [5, 11] and multidomain structures [6, 8].

Theoretical investigations of such systems have a long history [12] and a large number of results on the magnetic states (mostly within simplified models and by numerical methods) have been obtained [12, 13, 14]. However, these findings were often restricted to specific values of magnetic parameters and led to conflicting conclusions about the evolution of the magnetic states in these system. In particular, the understanding of the phenomena called *surface spin-flop* remained controversial [13]. Recently, we have achieved a complete overview on all one-dimensional solutions for the basic phenomenological model of antiferromagnetic superlattices with even number of layers N [7], and the magnetization processes in the limits of zero [8] and strong [11] uniaxial anisotropy have been investigated. In this paper, we systematize and discuss the results of [7, 8, 11, 15] giving a consistent description of magnetic states and their evolution in an applied magnetic field. Magnetization processes have been investigated in detail and corresponding phase diagrams are derived. These reveal the qualitatively different behaviour arising for low, high, and intermediate

*Corresponding author IFW Dresden, Postfach 270116, D-01171 Dresden, Germany. Tel.: +49-351-4659-542; Fax: +49-351-4659-537 ;
Electronic address: u.roessler@ifw-dresden.de

†Electronic address: bogdanov@kinetic.ac.donetsk.ua

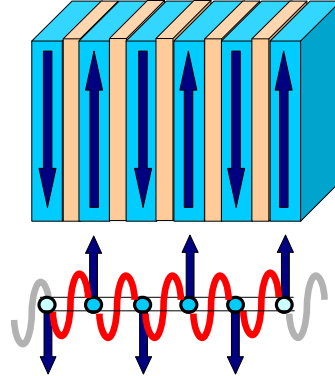


FIG. 1: The magnetic states of an antiferromagnetic superlattice stack can be represented by a linear chain of unity spins; the “exchange springs” are cut at the ends of the finite chain.

uniaxial anisotropy. A “dimerization” transformation for the energy of an antiferromagnetic superlattice with N layers into a chain of $N/2$ interacting “antiferromagnets” explains the physics ruling the magnetic phases in these nanostructures in the low anisotropy limit. The approach elucidates the crucial role of the *cut exchange* for the formation of magnetic states in an antiferromagnetic layer [16] and for the structure of the possible phase-diagrams in finite antiferromagnetic multilayer stacks [7]. At high anisotropies, the phase diagrams display a fixed sequence of metamagnetic transitions between collinear magnetic configurations. This simplicity of the phase structure of this micromagnetic model in the limiting cases allows to understand the general behaviour of its phase diagrams. Our results resolve the puzzle of reorientation transitions in these systems, which have been discussed as “surface spin-flop” for many years.

2. General model and simplifications.

Following [7, 8], an antiferromagnetic superlattice is described by a stack of N ferromagnetic plates with magnetizations \mathbf{m}_i , antiferromagnetic couplings, and N even. To calculate the one-dimensional configurations, one can replace this by a linear chain of coupled unity vector spins $\mathbf{s}_i = \mathbf{m}_i/|\mathbf{m}_i|$. For the system with uniaxial magnetic anisotropy its phenomenological energy can be written as

$$\Phi_N = \sum_{i=1}^{N-1} \left[J_i \mathbf{s}_i \cdot \mathbf{s}_{i+1} + \tilde{J}_i (\mathbf{s}_i \cdot \mathbf{s}_{i+1})^2 \right] - \mathbf{H} \cdot \sum_{i=1}^N \mathbf{s}_i - \frac{1}{2} \sum_{i=1}^N K_i (\mathbf{s}_i \cdot \mathbf{n})^2 - \sum_{i=1}^{N-1} K'_i (\mathbf{s}_i \cdot \mathbf{n}) (\mathbf{s}_{i+1} \cdot \mathbf{n}). \quad (1)$$

Here, J_i and \tilde{J}_i are bilinear and biquadratic exchange constants, respectively. The unity vector \mathbf{n} points along the common anisotropy axis; K_i and K'_i are constants of in-plane and inter-planar anisotropy.

For a detailed discussion of the model (1), its limits and relations to other theories, see [8, 15]. The functional (1) includes all main energy contributions which are known to play a noticeable role in these nanostructured systems. It can be used for a detailed description of specific systems and for the analysis of experimental data. Among the different magnetic interactions in (1), there are two factors which cause the striking behaviour of this class of magnetic nanostructures: (i) *uniaxial* anisotropy and (ii) *cut exchange bonds* [7]. Anisotropy is mandatory for field-driven reorientation. The second effect is illustrated in Fig. 1: interior layers are coupled to two neighbours, while the endmost layers interact only with one. The corresponding weakening of the exchange stiffness at the ends of the chain, the *cut exchange bonds* at the boundary layers, determines the reorientational effects. In principle, the same effect of cut exchange bonds rules the magnetization processes of a geometrically confined antiferromagnet with non-compensated surfaces. Similar effects cannot arise in *ferromagnetically* coupled multilayers (or ferromagnetic films) because here reorientational processes do not depend on the relative strength of the exchange interaction between the layers at the surface or in the interior.

The effects of uniaxial anisotropy and the exchange cut can be described by a simplified version of the model (1) with $J_i = J$, $K_i = K$, and $\tilde{J}_i = K'_i = 0$ for $i = 1$ to N . The vectors \mathbf{s}_i can be confined to a plane, which includes the

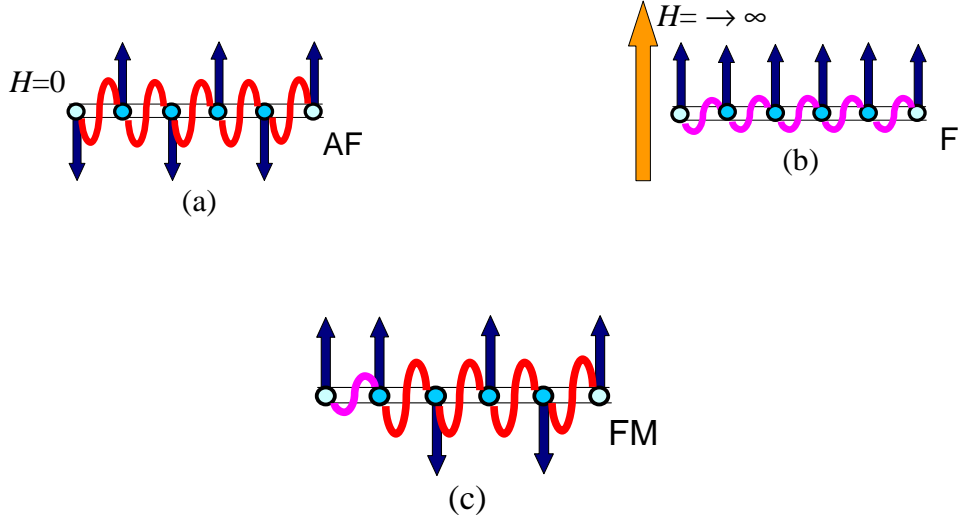


FIG. 2: Basic configurations: (a) antiferromagnetic ground state, (b) saturated state in large fields, and (c) ferrimagnetic states (FM) for large anisotropy at intermediate fields.

easy axis \mathbf{n} . For an applied field in direction of the easy axes, $\mathbf{H} \parallel \mathbf{n}$, the energy reads

$$\tilde{\Phi}_N = J \sum_{i=1}^{N-1} \cos(\theta_i - \theta_{i+1}) - H \sum_{i=1}^N \cos \theta_i - \frac{K}{2} \sum_{i=1}^N \cos^2 \theta_i, \quad (2)$$

where θ_i is the angle between \mathbf{s}_i and \mathbf{n} , and for $K > 0$ the axis \mathbf{n} is the easy direction of the magnetization.

The model (2) for the magnetic energy was introduced by Mills for a semi-infinite chain [12], and it has been studied in many works (see [13] and bibliography in [15]). This model, called here *Mills model*, is a basic model to discuss magnetic properties of antiferromagnetic superlattices. In the following sections we consider the structure of solutions for (2).

3. Special cases of Mills model.

In Eq. (2) there are three independent control parameters: number of the layers N , and the ratios H/J and K/J . We represent this phase space of the model by $(H/J, K/J)$ diagrams for different values of N . We start the analysis of Mills model from the limits of the control parameters, where the system becomes simple.

Limiting values of the field H . In these phase diagrams the (zero-field) ground state is always the *antiferromagnetic* phase (AF) with $\theta_{2i-1} = \pi$ and $\theta_{2i} = 0$ (Fig. 2(a)). At high field ($H \rightarrow \infty$) the minimum of the energy (2) corresponds to the *ferromagnetic* state (F) with $\theta_i = 0$ (Fig. 2(b)).

The two limits of N . For the simplest antiferromagnetic layer $N = 2$, the energy (2) reduces to that of a classical bulk two-sublattice antiferromagnet

$$\tilde{\Phi}_2 = J \cos(\theta_1 - \theta_2) - H(\cos \theta_1 + \cos \theta_2) - \frac{K}{2}(\cos^2 \theta_1 + \cos^2 \theta_2). \quad (3)$$

The corresponding phase diagram is plotted in Fig. 3. For $K < J$ a first-order transition between AF ($\theta_1 = 0$, $\theta_2 = \pi$) and the *spin-flop* (SF) ($\theta_1 = -\theta_2$) phase occurs at $H_{SF} = \sqrt{K(2J - K)}$. This is the *spin-flop* transition [17]. In the SF phase $\cos \theta_1 = H/H_F$, where $H_F = 2J - K$ is the field of the continuous (second-order) transition into the ferromagnetic phase. The critical fields $H_1 = \sqrt{K(2J + K)}$, $H_2 = H_F \sqrt{K/(2J + K)}$ are stability limits for the AF and SF phase, correspondingly. For $K > J$ the first-order transition between AF and ferromagnetic phases (*metamagnetic* phase transition) occurs at the critical field $H_{FM} = J$. For this transition the continuation of the line $H_F(K)$ gives the stability limit of the ferromagnetic phase. In multilayers with $N > 2$ the exchange coupling per any internal layer is $2J$. Thus, the phase diagram for the systems with very large N can be obtained from that for $N = 2$ by substitution $J \rightarrow 2J$. These critical lines are shown in Fig. 3. This procedure does not yield a completely correct phase diagram because one neglects the cut of exchange bonds at the boundaries.

High and low anisotropy. Sufficiently large anisotropy suppresses deviations of the magnetization from the easy directions. In this limit, only phase transitions between the collinear states are possible [11]. In particular for Mills

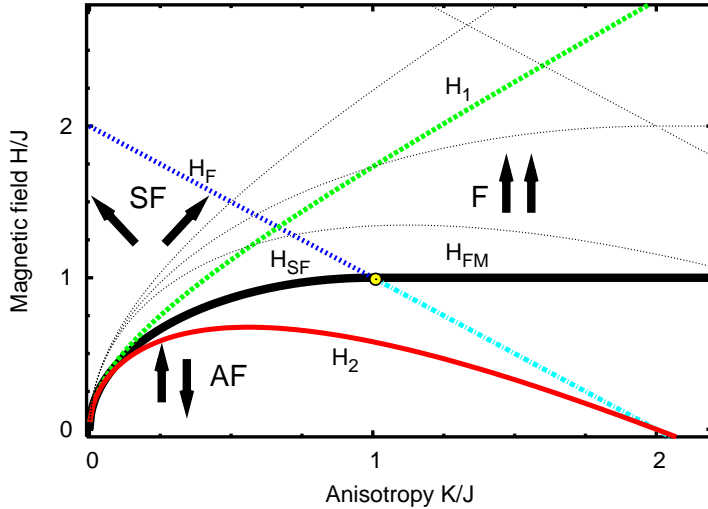


FIG. 3: Phase diagram for two antiferromagnetically coupled uniaxial layers $N = 2$, or equivalently a two-sublattice bulk antiferromagnet [17], with field along easy axis. Light grey lines give transition lines, rescaled by $J \rightarrow 2J$, as approximation for phase diagrams of multilayer systems $N \rightarrow \infty$.

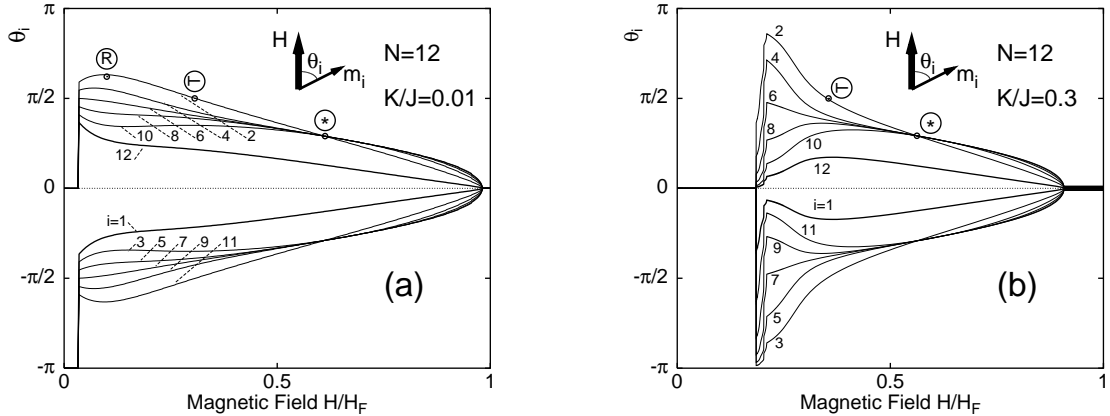


FIG. 4: Evolution of configuration profiles for Mills model $N = 12$ with low anisotropy (a) and for intermediate anisotropies (b) with field along the easy axis. In the SF-phase in (a) some moments rotate against the external field, e.g. moment 2, up to point (R); at (⊥) it is perpendicular to the field. At point (*), projections of all interior moments onto the field are equal. With stronger anisotropy, a series of canted and asymmetric configurations occurs between AF and SF-state.

model there are two phase transitions [13, 16]: at $H_{FM} = J$ between AF and *ferrimagnetic* (FM) phases with a flipped pair of moments (Fig. 2(c)) and at $H_{FM2} = 2J$ between FM and the ferromagnetic state. The transition from the AF-phase into the collinear FM states is again a consequence of the exchange cut. The moment at the surface pointing against the field can be reversed more easily than a moment in the interior. However, the realizations of the ferrimagnetic phases are degenerate for Mills model. They are built from one pair of ferromagnetically aligned spins $\uparrow\uparrow$ between two collinear antiferromagnetic domains, so that the two endmost moments point in direction of the field: $(\uparrow\downarrow \dots \uparrow\downarrow) \uparrow\uparrow (\downarrow\uparrow \dots \downarrow\uparrow)$. All configurations with different location of the ferromagnetic pair, equivalently with different lengths of the two adjoining antiferromagnetic domains, have the same energy for Mills model Eq. (2). Therefore, they have the same transition fields H_{FM} and H_{FM2} for the first-order transitions into the antiferromagnetic ground state and into the ferromagnetic phase, respectively. However, their stability regions are different and depend on N . This remarkable degeneracy is due to the highly symmetric choice for the materials constants of individual layers in energy (2). It does not hold for general cases described by Eq. (1) [11].

Next, we consider the opposite limit of low anisotropy. Due to the *cutting of exchange bonds* the SF phase in the systems with $N > 2$ has an inhomogeneous structure across the stack and it undergoes a complex evolution in an applied magnetic field [7, 8]. An example is shown in Fig. 4(a). For the highly symmetric Mills model this spin-flop

state preserves mirror symmetry about the center of the layer, $\theta_i = -\theta_{N+1-i}$. For stronger anisotropies, such an inhomogeneous spin-flop state is reached only at higher fields, see Fig. 4(b).

4. $H-K$ phase diagram for Mills model.

A phase diagram for an antiferromagnetic superlattice is shown in Fig. 5 as representative for all cases. At large

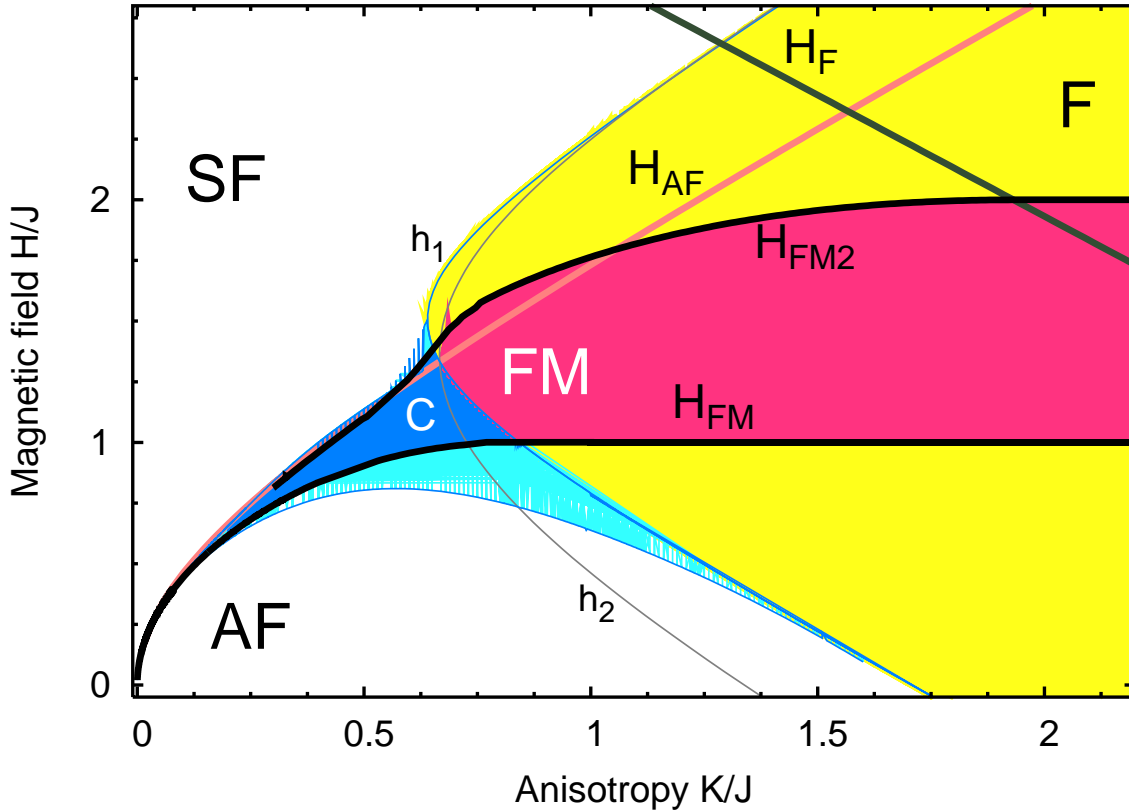


FIG. 5: Phase diagram Mills model Eq. (2) with $N = 12$ layers representative for phase structures of uniaxial antiferromagnetic superlattices with field along easy axis. The collinear ferrimagnetic states are stable in the shaded region FM. First-order transitions occur at lines H_{FM} and H_{FM2} . Lines h_1 and h_2 are stability limits of different FM-phases. Canted asymmetric phases exist in region C, which is grossly simplified here. Lighter shaded areas mark metastability limits of FM- and C-phases. Line H_F : continuous transition between spin-flop and saturated phase, and stability limit of F below line H_{FM2} .

anisotropies, one has the simple sequence of collinear phases $AF \rightarrow FM \rightarrow F$ separated by first-order (metamagnetic) transitions. The special line H_{AF} is the stability limit of the AF-phase. For Mills model, one has $H_{AF} = \sqrt{2JK + K^2}$ for all $N \geq 4$ and even [13]. In Fig. 5 stability limits for two realizations of the FM-phases are shown: h_1 for phase $FM_1 = (\uparrow\downarrow\dots)\uparrow\uparrow$ with the ferromagnetic pair at the surface, h_2 for $FM_2 = (\uparrow\downarrow\dots)\uparrow\uparrow(\downarrow\uparrow)$. Thus, at intermediate anisotropies the collinear FM-phases can be distorted elastically. These are canting instabilities. The transitions between the collinear phase FM_i and a corresponding canted phase C_i usually are continuous. These instabilities lead to the appearance of series of different asymmetric phases in the region marked “C” in Figs. 5 and 7. A typical evolution through this region is demonstrated in Fig. 6, there are series of first-order transitions between various canted phases. The low anisotropy and low-field part of the phase diagram in Fig. 7 is shown with respect to the stability limit H_{AF} . For small anisotropies below point b, there is only the spin-flop transition $AF \rightarrow SF$. Finally, the SF-phase reaches the saturated F-state continuously at the straight line $H_F = H_e^{(N)} - K$ with an exchange field H_e depending on N (Fig. 5).

5. Does a surface spin-flop occur in antiferromagnetically coupled multilayers?

a. *Recent picture of a surface spin-flop.* A common scenario for reorientational transitions in antiferromagnetic multilayers (see [4, 14]) was built on the basis of analytical investigations for low anisotropy systems [12] and numerical simulations for systems with higher anisotropy [2, 13]. It is described as a local instability driven by the field at the surface of the uniaxial antiferromagnet with a moment pointing against the direction of the field. This should create a flopped configuration at this surface, hence, an asymmetric state. This picture seems to be born out by the evolution through sequences of canted phases as shown in Fig. 6 for systems with sizeable anisotropy. But, it is not completely

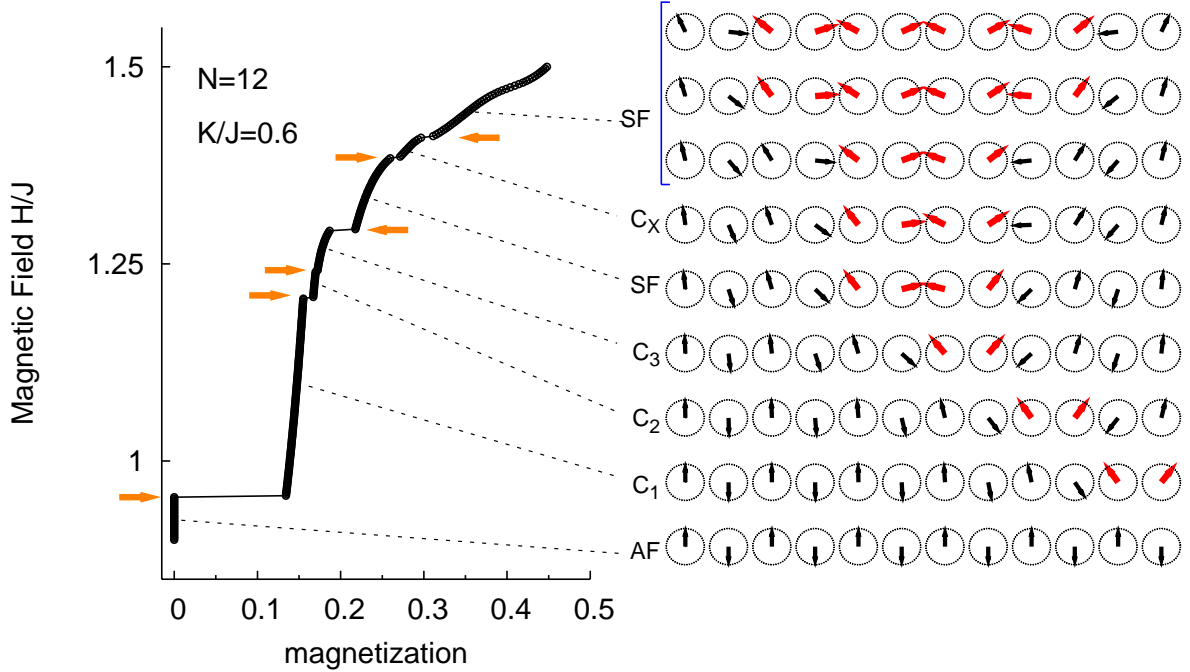


FIG. 6: Evolution of equilibrium magnetic states for Mills model with $N = 12$ layers in the region of canted phases. From bottom to top a series of transition leads from antiferromagnetic to spin-flop phase with increasing field. Left panel: magnetization (first-order transitions are marked by arrows). Right panel: corresponding configurations.

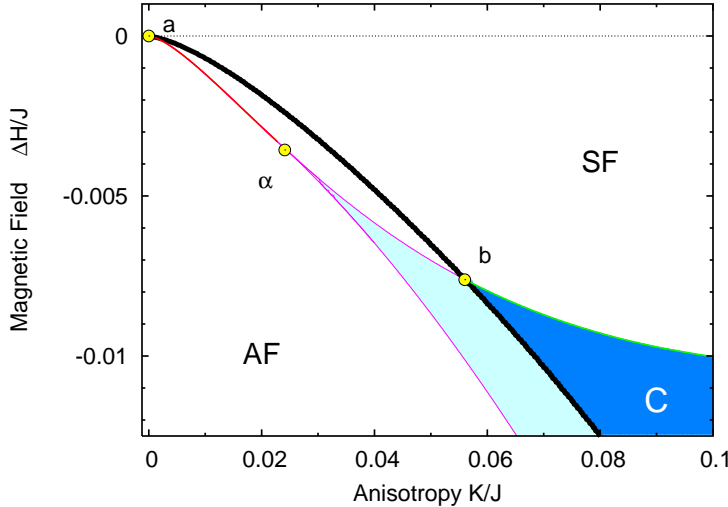


FIG. 7: Low-anisotropy and low-field part of the $N = 12$ phase diagram in Fig. 5. Magnetic field is given relative to the metastability field of AF-phase $\Delta H = H_{\text{AF}} - H$. First-order transitions take place at the thick black line: from AF to SF-phase between points a and b; for larger anisotropy beyond point b, from AF to C_1 -phase (see Fig. 6). In the dark area the canted phase C_1 is stable, the lighter shaded area is its metastability range beyond the first-order transition line. Point α is the low anisotropy limit, where the C_1 -phase is metastable.

correct. The transition field for the surface spin-flop was identified with the instability field of the antiferromagnetic phase $H_{\text{AF}} \simeq \sqrt{2JK}$ [2, 12]. With increasing field, this flopped configuration “moves” into the center of the stack and finally the flopped configurations should expand by another transition at the field for the bulk spin-flop $H_B \simeq \sqrt{4JK}$. Therefore, the ratio $\sqrt{2}$ between the field for this “surface spin-flop” and the bulk spin-flop should hold. The first-order transition AF \rightarrow C_1 clearly resembles an isolated flop at the surface. However, it has to take place considerably below H_{AF} (see Fig. 6). The anomalies identified with the “bulk spin-flop” are related to complicated canting instabilities

at fields below H_B (transitions between SF and C_x in Fig. 6).

b. *The spin-flop in the low anisotropy limit.* The picture of the “surface spin-flop” also is incomplete. There are no asymmetric phases or isolated flopped configurations at the surface of a multilayer with low anisotropy (Fig. 7).

For low anisotropy systems ($K \ll J$) and weak magnetic fields ($H \ll J$) the energy (2) can be reduced to a model which allows to extract the physical mechanism behind the complex and unusual reorientational processes described in the previous sections. Following a standard procedure we introduce for a two-layer system with (3) the vector of the net magnetization $\mathbf{M} = (\mathbf{s}_1 + \mathbf{s}_2)/2$ and staggered vectors $\mathbf{L} = (\mathbf{s}_1 - \mathbf{s}_2)$, for each antiferromagnetic pair. From $\mathbf{s}_i = 1$ follows that $M^2 + L^2 = 1$ and $\mathbf{M} \cdot \mathbf{L} = 0$. Using these equations the energy (3) can be written as a function of $|\mathbf{M}|$ and the angle ϕ between \mathbf{L} and the easy axis. After minimization with respect to $|\mathbf{M}|$ the energy can be reduced to the following form

$$\tilde{\Phi}_2 = -\frac{H^2 - 2JK}{4J} \cos 2\phi. \quad (4)$$

Compared to the energy (3) the Eq. (4) includes only leading contributions with respect to the small parameters K/J , H/J . In this limit the spin-flop field and lability fields of AF and SF phases become equal ($H_{SF} = H_1 = H_2 = \sqrt{2JK}$). This equation clearly demonstrates the competing character of the magnetic states in a bulk two-sublattice easy-axis antiferromagnet and the physical essence of the spin-flop transition. The uniaxial anisotropy stabilizes the AF phase with the staggered vector along the easy-axis while the applied field favours the flopped states with $\mathbf{L} \perp \mathbf{n}$. At the threshold *spin-flop* field $H_{SF} = \sqrt{2JK}$ the system switches from one mode to another.

Now we simplify the energy of the superlattice with N layers considering it as a system of interacting *dimers*. We sort N magnetic moments in the chain into $N/2$ pairs: $(\mathbf{s}_1, \mathbf{s}_2)$, $(\mathbf{s}_3, \mathbf{s}_4)$, ..., $(\mathbf{s}_{2j-1}, \mathbf{s}_{2j})$, ..., $(\mathbf{s}_{N-1}, \mathbf{s}_N)$ with $j = 1, \dots, N/2$. The chain of spins for the magnetic moments then appears as a chain of *dimers*, and each of these can be considered as a two-sublattice antiferromagnet. Net magnetization $\mathbf{M}_j = (\mathbf{s}_{2j-1} + \mathbf{s}_{2j})/2$ and staggered vectors $\mathbf{L}_j = (\mathbf{s}_{2j-1} - \mathbf{s}_{2j})/2$ are introduced for each antiferromagnetic pair; from $\mathbf{s}_i = 1$, one now has $M_j^2 + L_j^2 = 1$ and $\mathbf{M}_j \cdot \mathbf{L}_j = 0$. For $H, K \ll J$ the net magnetization is always small, $\mathbf{M}_j \ll 1$. Thus, after expanding (2), one can use an independent minimization with respect to the variables \mathbf{M}_j .

$$\tilde{\Phi}_N = \frac{J}{2} \sum_{j=1}^{N/2-1} (\phi_{j+1} - \phi_j)^2 - \sum_{j=1}^{N/2} \frac{H^2 - \Lambda_j K}{2\Lambda_j} \cos 2\phi_j + \Xi(\phi_j). \quad (5)$$

From the minimization the net magnetizations are fixed as dependent parameters by $M_j = H \sin \phi_j / \Lambda_j$. The constants are $\Lambda_1 = \Lambda_{N/2} = 3J$ for the pairs at the surfaces, and $\Lambda_j = 4J$ for the interior of the stack, $j = 2, \dots, N/2 - 1$. The last contribution in (5) is a “surface”-term given by

$$\Xi(\phi_j) = -J(\Lambda_2^{-1} + \Lambda_1^{-1})(\mathbf{H} \cdot \mathbf{l}_1 - \mathbf{H} \cdot \mathbf{l}_{N/2}) - J(\Lambda_2^{-1} - \Lambda_1^{-1})(\mathbf{H} \cdot \mathbf{l}_2 - \mathbf{H} \cdot \mathbf{l}_{N/2-1}), \quad (6)$$

where $\mathbf{l}_j = \mathbf{L}_j/|\mathbf{L}_j|$ are unity vectors along the staggered magnetization. The energy contribution (6) is explicitly given by $\Xi(\phi_j) = -7H(\cos \phi_1 - \cos \phi_{N/2})/12 + H(\cos \phi_2 - \cos \phi_{N/2-1})/12$. Comparison between the energies $\tilde{\Phi}_2$ (4) and $\tilde{\Phi}_N$ (5) helps to understand the different character of reorientational transitions in the antiferromagnetic chain.

Eq. (5) can be considered as the energy of the interacting *dimers* with “self-energy” (4). The first term in (5) has the form of an elastic energy arising from the exchange coupling between *dimers*. The second is a potential energy, which changes its wells at critical values of the field $H = \sqrt{\Lambda_j K}$. There are two different critical fields: $H_S = \sqrt{3JK}$ for the surfaces, while in the interior one has $H_B = \sqrt{4JK}$. The two fields H_S and H_B would correspond to independent spin-flops of the antiferromagnetic pairs either at the surface or in the bulk in the absence of couplings along the chain.

Clearly, H_S is an upper limit for an instability of the AF-state in a finite superlattice. It would correspond to a “true surface spin-flop”. But the transition from AF to SF is driven by the energy contribution from the antisymmetric “surface”-terms Ξ Eq. (6), which describe the effect of the cut exchange. This contribution becomes negative when the staggered vectors at both ends of the chain, \mathbf{l}_1 and $\mathbf{l}_{N/2}$, are antiparallel. Thus, before reaching the field H_S , a configuration resembling a 180-degree antiferromagnetic domain wall will be created in the chain. The symmetry of the energy terms in (5) only allows (mirror) symmetric configurations. These are the symmetric SF-state (Fig 4(a)). In multilayers with large N the SF-configuration may appear as a rather localized wall-like structure in the center of the system between antiferromagnetic domains with antiparallel staggered vectors. In this state reaching the field H_B , the antiferromagnetic configuration of the interior antiferromagnetic pairs must change. Asymptotically with $N \rightarrow \infty$, this is the approach to the classical spin-flop for the corresponding infinite bulk antiferromagnet (Fig. 3).

Thus, we have the following important conclusion. The reorientational transitions in these confined antiferromagnets known as *surface spin-flop* are not related to *surface* states, and they are no *spin-flops*. It is a transition between the

AF and the inhomogeneous spin-flop phase induced by the instability of the antiparallel magnetization in the endmost layers owing to the exchange cut. It is not related to the competition between the applied magnetic field and the uniaxial anisotropy as in bulk antiferromagnets. Owing to the elastic couplings of the system, there is no magnetic transition related to the “bulk” threshold field H_B for finite superlattices. However a strong magnetic anomaly may be observable near H_B .

6. Conclusions.

We have demonstrated a fundamental difference of the spin-flop behaviour in multilayers with low anisotropy and with higher anisotropy. At low anisotropy, there is only an inhomogeneous symmetric spin-flop phase with a wall-like configuration in the center or somewhere below the surfaces. This should also hold for films made of usual antiferromagnetic materials where $K/J \ll 1$. This result explains the failure to observe a surface spin-flop as a state nucleated at surfaces of antiferromagnetic layers. Canted asymmetric states, which show a flopped configuration at the surface, are observed in multilayers with larger anisotropies [2, 4]. Metamagnetic transitions are found in antiferromagnetic multilayers with strong perpendicular anisotropy[5]. By an extension of our results for the generic Mills model, an analysis of the general models (1) is feasible. Their phase diagrams can be similarly partitioned into the three characteristic regions: at low anisotropies there is a sequence $AF \rightarrow SF \rightarrow F$ -phase with an inhomogeneously distorted SF-phase; at high anisotropies cascades of metamagnetic transitions between collinear phases take place [11]. Number and structure of these collinear phases determine the intermediate region of the phase space, where canting instabilities occur and asymmetric transitional phases appear. In this region, the phase diagrams may still reflect some features described as “surface spin-flop”[2]; however, new types of magnetic states may be stabilized and complicated magnetization processes will arise when the particular degeneracy of Mills model is lifted.

Acknowledgments A. N. B. thanks H. Eschrig for support and hospitality at the IFW Dresden.

[1] P. Grünberg, et al., *Phys. Rev. Lett.* **57**, 2442 (1986).
[2] R. W. Wang, D. L. Mills, E. E. Fullerton, J. E. Mattson, S. D. Bader, *Phys. Rev. Lett.* **72**, 920 (1994).
[3] V. V. Ustinov, et al., *J. Magn. Magn. Mater.* **226-230**, 1811 (2001); V. Lauter-Pasyuk, et al., *Phys. Rev. Lett.* **89**, 167203 (2002); V. Lauter-Pasyuk, et al., *J. Magn. Magn. Mater.* **258-259**, 382 (2003).
[4] S. G. E. te Velthuis, J. S. Jiang, S. D. Bader, G.P. Felcher, *Phys. Rev. Lett.* **89**, 127203 (2002).
[5] O. Hellwig, et al., *Nature Materials* **2**, 112 (2003).
[6] D. L. Nagy, et al., *Phys. Rev. Lett.* **88**, 157202 (2002).
[7] U. K. Rößler and A. N. Bogdanov, *Phys. Rev. B* **87**, 094405 (2004).
[8] U. K. Rößler and A. N. Bogdanov, *Phys. Rev. B* **69**, 184420 (2004).
[9] G. J. Strijkers, S. M. Zhou, F. Y. Yang, and C. L. Chien, *Phys. Rev. B* **62**, 13896 (2000); K. Y. Kim, et al., *J. Appl. Phys.* **89**, 7612 (2001).
[10] E. E. Fullerton, et al., *IEEE Trans. Mag.* **39**, 639 (2003); A. Moser, et al., *J. Phys. D* **35**, R157 (2002).
[11] U. K. Rößler and A. N. Bogdanov, *J. Magn. Magn. Mater.* **240**, 539 (2004).
[12] D. L. Mills, *Phys. Rev. Lett.* **20**, 18 (1968); D. L. Mills and W. M. Saslow, *Phys. Rev.* **171**, 488 (1968); F. Keffer and H. Chow, *Phys. Rev. Lett.* **31**, 1061 (1973).
[13] L. Trallori, et al., *Phys. Rev. Lett.* **72**, 1925 (1994); S. Rakhmanova, D. L. Mills, and E. E. Fullerton, *Phys. Rev. B* **57**, 476 (1998); N. Papanicolaou, *J. Phys.: Condens. Matter* **10**, L131 (1998); M. Momma and T. Horiguchi, *Physica A* **259**, 105 (1998); A. L. Dantas and A. S. Carriço, *Phys. Rev. B* **59**, 1223 (1999); C. Micheletti, R. B. Griffiths, and J.M. Yeomans, *Phys. Rev. B* **59**, 6239 (1999).
[14] D. L. Mills, *J. Magn. Magn. Mater.* **198-199**, 334 (1999).
[15] U. K. Rößler and A. N. Bogdanov, to be published.
[16] A. N. Bogdanov, U. K. Rößler, *Phys. Rev. B* **68**, 012407 (2003).
[17] L. Néel, *Annales de Physique* **5**, 232 (1936).